Int. J. Heat Mass Transfer. Vol. 30, No. 3, pp. 449–458, 1987
Printed in Great Britain

0017–9310/87 $3.00 + 0.00
Pergamon Journals Ltd.

Direct contact condensation of superheated steam on water

G. P. CELATA, M. CUMO, G. E. FARELLO and G. FOCARDI
ENEA—TERM/ISP Casaccia, Via Anguillarese 301, 00060 Rome, Italy

(*Received* 22 *April* 1986)

Abstract—Referring to the interaction of superheated steam (practically stagnant) with subcooled water (slowly moving) the results of an experimental research are presented and discussed. As foreseen in a theoretical investigation, the total thermal power (and consequently the total heat transfer coefficient) does not show an appreciable dependence on superheated steam temperature, so it can be practically evaluated by means of available correlations for saturated steam conditions. The direct contact condensation heat transfer coefficient is linked to the overall one and is slightly dependent on the degree of steam superheating, as experimentally confirmed.

1. INTRODUCTION

THE POSSIBLE interaction between steam and liquid inside the reactor pressure vessel, following a postulated loss-of-coolant accident and consequent emergency core cooling system intervention, happens—from a thermodynamic viewpoint—with the steam in saturated or superheated conditions and the water in subcooled conditions (with reference to the system pressure).

A previous experiment, related to the interaction between saturated steam (in a quasi-stagnant condition) and subcooled water (with a low interfacial velocity) [1], permitted the analysis, in the frame of the investigated ranges, of the influence on the direct contact condensation heat transfer coefficient of the main parameters involved in the phenomenon (system pressure, water and steam temperatures, water mass flow rate).

Although direct contact interaction between saturated steam and water has met with an appreciable amount of attention in the international scientific community [2–14], the phenomenon linked to the thermodynamic conditions of superheated steam have not yet been sufficiently investigated.

This paper deals with the results of an experiment that aimed to investigate the direct interaction between superheated steam and stratified, slowly moving water; such conditions allow the elimination of any mechanical or fluid-dynamics influence on the direct contact heat transfer coefficient. A theoretical dissertation is presented before the experimental results.

2. EXPERIMENTAL APPARATUS

A schematic diagram of the experimental apparatus is shown in Fig. 1. The apparatus includes, besides the test section, a water storage tank, an electric heater for water heating (10 kW), an electric boiler for saturated steam production (15 kW; 20 kg h^{-1}) and an electric heater for steam superheating.

The loop characteristics are:

pressure	up to 10 bar
water mass flow rate, W_i	up to 120 kg h^{-1}
steam mass flow rate	up to 20 kg h^{-1}
inlet saturated steam temperature, T_{sat}	up to 160°C
inlet water temperature, T_i	up to 80°C
inlet superheated steam temperature, T_{vsh}	up to 200°C

The test section (Fig. 2) is made up of a cylindric vessel with a flange at the bottom. A Teflon pool in which the water is allowed to flow radially is placed on the flange. Water is introduced from the bottom of the pool through 12 distribution holes along a circumferential distribution and, after the interaction with the steam, exits through a central discharge channel in order to be collected and 'processed' to get an evaluation of the condensed mass flow rate.

The water discharge channel is kept 8 mm below the water surface, so as to prevent steam leakages.

The water surface level is kept strictly constant over all the tests; this kind of situation enables a simple defined geometry to be considered (a cylinder whose diameter is the pool inner diameter and whose height is the distance between the water level and the water discharge channel) inside which the water may be supposed to flow horizontally and parallel to the water surface.

Steam is introduced from the top of the test section in order to get rid of the convective heat transfer component.

Measurement of the thermal field inside the pool, together with inlet and outlet water temperature, and inlet steam temperature as well, have been performed by employing K-type thermocouples ($D = 0.8$ mm).

NOMENCLATURE

A, B	integration constants
c_{pl}	liquid specific heat at constant pressure
c_{pv}	vapour specific heat at constant pressure
D	diameter
h	heat transfer coefficient
H	enthalpy
K	thermal conductivity
l	length
p	pressure
P	thermal power
q''	heat flux
R	thermal resistance
S	heat transfer surface, cross-section
$T, \Delta T$	temperature, temperature difference
v	steam velocity
W	mass flow rate
x	coordinate.

Subscripts

b	bulk
c	condensation, condensed
i	inlet
o	outlet
sat	saturation
t	total
v	steam
vsat	saturated steam.

Greek symbols

α	thermal diffusivity
λ	latent heat
ρ	density.

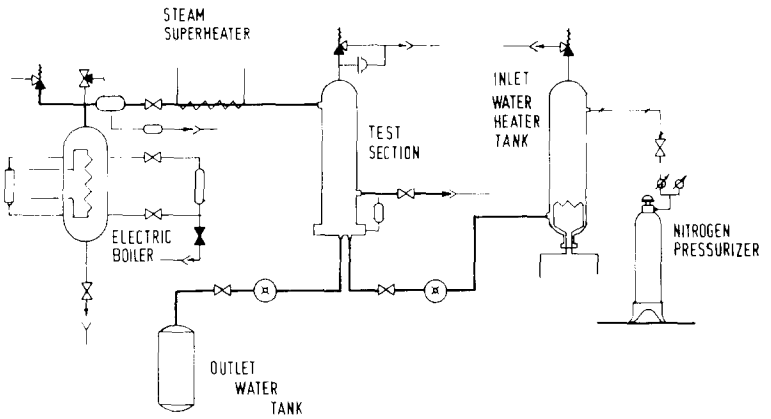

FIG. 1. Schematic diagram of the experimental loop.

The water temperature profile clearly indicates that the bulk water is at a uniform temperature called 'bulk temperature', T_b, very close to the inlet temperature, T_i.

The steam-side thermal field has also been measured with a K-type thermocouple ($D = 0.5$ mm) to detect the temperature gradient in the de-superheating zone. The water mass flow rate has been measured by means of turbine flow meters. The inner diameter of the test section vessel is 160 mm, whilst the pool diameter, D, is 100 mm.

3. THEORETICAL CONSIDERATIONS

Considering the interaction between superheated steam (quasi-stagnant) and subcooled water with very low interfacial velocities (2–5 cm s^{-1}), and referring to a steady-state condition, the thermal power transferred from the steam to the liquid phase can be determined by the three contributions:

(1) P_d, thermal power due to steam de-superheating;
(2) P_c, thermal power due to condensation;
(3) P_s, thermal power due to condensed subcooling (to the outlet liquid temperature).

Supposing that the condensed mass flow rate, W_c, is known, then the three components of the total thermal power are expressed by

$$P_d = W_c(H_{vsh} - H_{vsat}) \quad (1)$$

$$P_c = W_c\lambda \quad (2)$$

$$P_s = W_c(H_{lsat} - H_o). \quad (3)$$

Steam moves perpendicularly towards the water surface with a low velocity (2–3 cm s^{-1}) so that pressure gradients and dynamic actions may be neglected. In addition, to use of degassed water and the presence of a non-condensable bleeder line just above the water surface allows the effects of non-condensable gas on

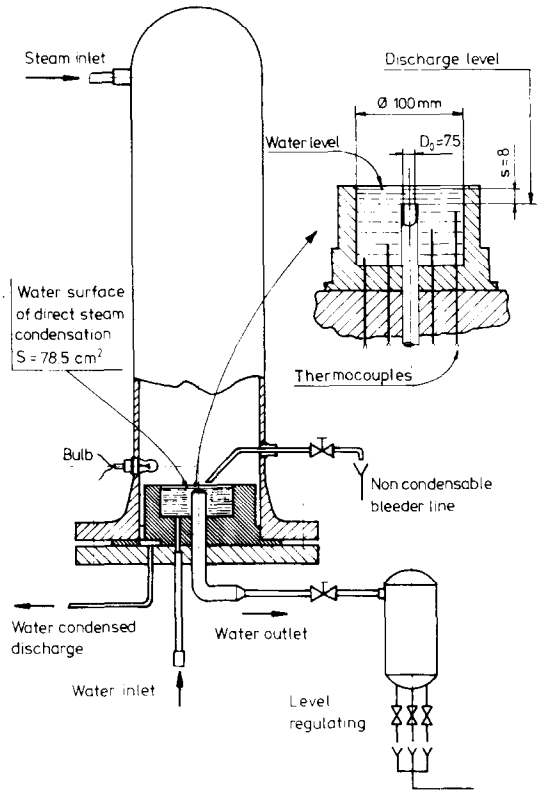

FIG. 2. Schematic diagram of the test section.

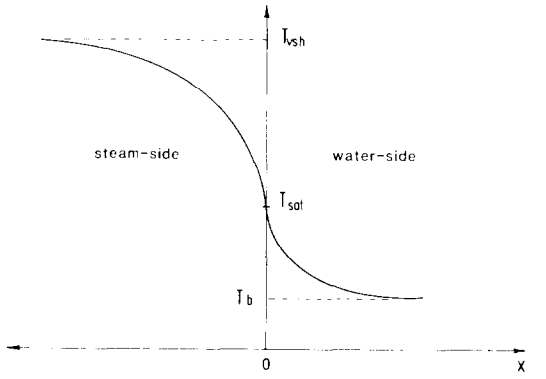

FIG. 3. Qualitative scheme of steam-side (left) and water-side thermal gradients (right).

the phenomenon to be neglected. As a last observation, it must be considered that the water surface quickly reaches the saturation temperature corresponding to the test section pressure.

Under these premises the water and steam-side thermal fields can be schematized, qualitatively, as shown in Fig. 3.

The energy transfer is linked to water and steam thermal resistances; the water capacity in heat removal depends on its physical properties (density, conductivity, specific heat, etc.) and on liquid flow characteristics (velocity, turbulence, etc.).

On the steam-side, only the power linked to the steam de-superheating has to be transferred.

We assume for the steam-side thermal field a one-dimensional hypothesis (thermal gradient normal to the heat transfer surface and lateral surfaces, limiting the steam, adiabatic) and the x-axis normal to the water surface with the origin on it and in the same direction as the heat flux.

Let us now take into consideration the infinitesimal rectangular cross-section steam-side volume element, having dx as a height, and a base surface of area equal to 1.

Indicating with v the steam velocity, uniform (parallel to the x-axis with the same direction) and with K_v, c_{pv} and ρ_v, the steam conductivity, specific heat and density, respectively, and assuming as positive the heat entering the control volume, the heat balance in steady-state conditions yields the equation

$$-\rho_v c_{pv} v \frac{\partial T}{\partial x} + K_v \frac{\partial^2 T}{\partial x^2} = 0. \tag{4}$$

Equation (4), solved with the average values of the physical properties, gives the steam-side temperature distribution

$$T(x) = A(\alpha_v/v)[\exp(v/\alpha_v)x] + B \tag{5}$$

where $\alpha_v = K_v/\rho_v c_{pv}$ is the steam thermal diffusivity.

Integration constants A and B have to be determined with the following boundary conditions:

(a) with the steam region wider than the zone characterized by the thermal gradient, we have

$$\lim_{x \to -\infty} T(x) = B = T_{vsh};$$

(b) the water surface temperature is the saturation temperature

$$T(0) = T_{sat} = A(\alpha_v/v) + B$$

and therefore

$$A = (T_{sat} - T_{vsh})v/\alpha_v.$$

Indicating with ΔT_{vsh} the difference between the superheating temperature, T_{vsh}, and the saturation value, T_{sat}, equation (5) becomes

$$T(x) = T_{vsh} - \Delta T_{vsh}[\exp(v/\alpha_v)x]. \tag{6}$$

Considering that, in the test section, the heat transfer surface, S, is coincident with the steam flow cross-section, the steam velocity can be expressed by

$$v = \frac{W_c}{\rho_v S} = \frac{P_c}{\rho_v S \lambda} = \frac{q_c''}{\rho_v \lambda} \tag{7}$$

where q_c'' is the condensation heat flux.

Finally for the steam-side temperature distribution we get

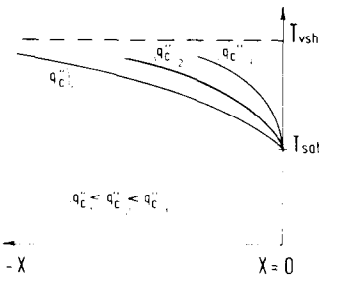

FIG. 4. Qualitative trend of steam-side temperatures vs condensation heat flux.

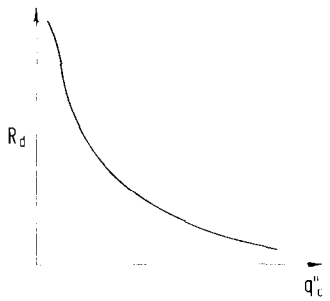

FIG. 5. Qualitative trend of steam-side thermal resistance, R_d, vs condensation heat flux.

$$T(x) = T_{vsh} - \Delta T_{vsh} \exp\left[\left(\frac{q''_c c_{pv}}{K_v \lambda}\right) x\right] \qquad (8)$$

the term $K_v\lambda/q''_c c_{pv}$ (dimensionally a length), may be defined as the 'de-superheating length', l_d, which gives an indication about the de-superheating region extension (the order of magnitude of l_d is a few mm).

Dividing l_d by the steam thermal conductivity, K_v, we have the steam-side thermal resistance expression

$$R_d = l_d/K_v = \lambda/q''_c c_{pv}.$$

Bearing in mind that c_{pv} is a slight function of the temperature (from 100 to 200°C the variation is less than 3%), for a fixed pressure, R_d depends only on condensation heat flux, q''_c. The heat flux is linked to the water heat transfer coefficient; consequently the layer thickness, inside which most of the de-superheating thermal jump occurs, varies and depends on water capacity in heat removal.

Practically the whole thermal phenomenon is governed by the water thermal resistance. In fact there is no effective resistance, steam-side, in energy transfer.

Figure 4 shows the qualitative trend of the steam-side temperature vs q''_c, whilst in Fig. 5 a typical R_d vs q''_c trend is plotted.

For the above considerations it can be concluded that the total thermal power exchanged (for surface unit) depends on saturation temperature, T_{sat}, inlet water temperature, T_i, inlet water mass flow rate, W_i, and liquid flow characteristics.

Therefore, if, for a fixed geometry, the total heat transfer coefficient, h_t, is known, then for the saturated steam condition, we can write

$$P_t = P_d + P_c + P_s = h_t S(T_{sat} - T_i). \qquad (9)$$

Using the given expressions of P_d, P_c and P_s, and resolving with respect to the condensed mass flow rate, W_c, we have

$$W_c = P_t/[\lambda + c_{pv}(T_{vsh} - T_{sat}) + c_{pl}(T_{sat} - T_o)]. \qquad (10)$$

As

$$P_c = W_c\lambda \cong h_c S(T_{sat} - T_i) \qquad (11)$$

for the direct contact condensation heat transfer coefficient, h_c, the following expression is obtained

$$h_c = \lambda h_t/[\lambda + c_{pv}(T_{vsh} - T_{sat}) + c_{pl}(T_{sat} - T_o)]. \qquad (12)$$

From equations (10) and (12) W_c and h_c turn out to be, from a theoretical point of view, dependent on superheating temperature.

4. TEST MATRIX

The main aim of the present experiment is to determine the heat transfer coefficient in direct contact condensation of superheated steam on subcooled water and to analyse its behaviour as a function of steam superheating. The test matrix used was:

saturated steam temperature, T_{sat} (°C): 105, 125, 155
system pressure, p (bar): 1.21, 2.32, 5.43
inlet water mass flow rate, W_i ($g\,s^{-1}$): 3.0, 6.0, 10.0, 16.0, 23.0, 30.0
inlet water temperature, T_i (°C): 20 and 70 (only for T_{sat} = 105°C)
superheated steam temperature, T_{vsh} (°C): up to 200°C with a step of 15°C starting from saturation conditions

for a total of 126 runs.

5. EXPERIMENTAL RESULTS AND DATA ANALYSIS

As far as the steam-side thermal field is concerned, Fig. 6 shows typical measured temperature distributions vs the distance from the water surface, compared with the predictions given by equation (5). The agreement between experimental data and theoretical predictions is appreciable.

In Fig. 7 the total thermal power, P_t, is plotted vs steam superheating, ΔT_{vsh}, for different values of inlet water mass flow rate and fluid thermodynamic conditions. From the analysis of such graphs no dependence of P_t on degree of steam superheating can be evidenced, as foreseen in the theoretical considerations presented in Section 3 (equation (9)). The total thermal power is, of course, a function of water

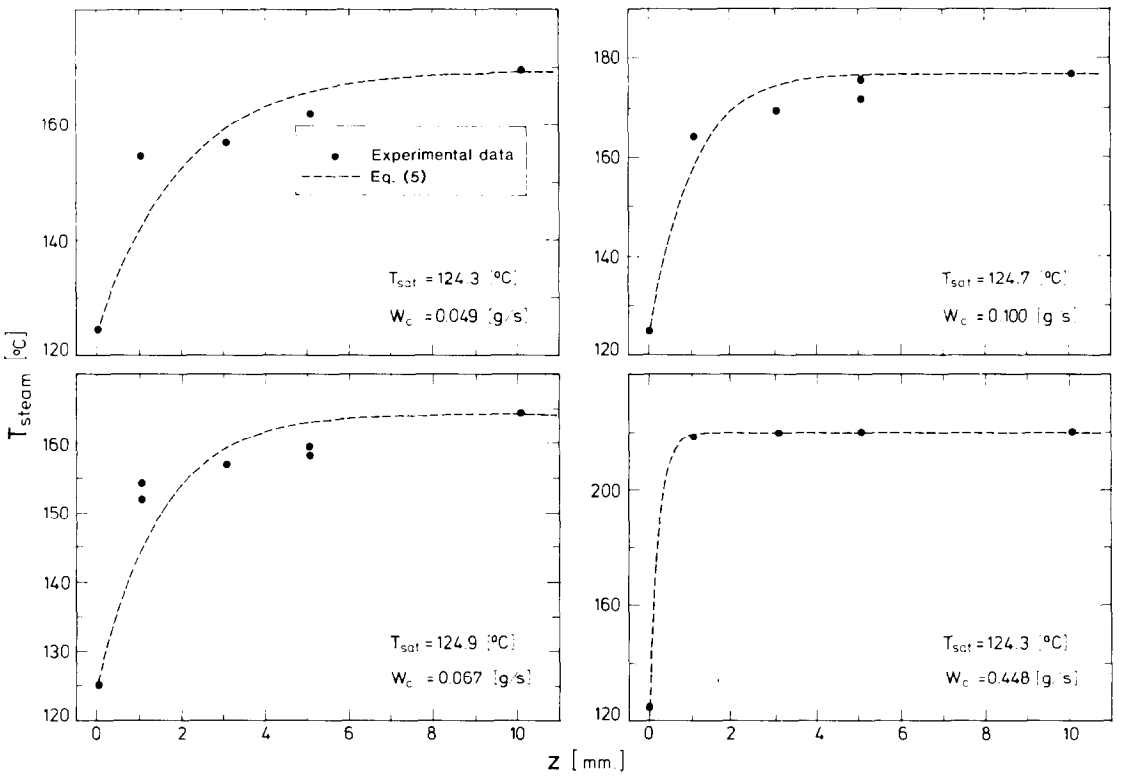

FIG. 6. Comparison between steam-side thermal gradient measurements and predictions from equation (5).

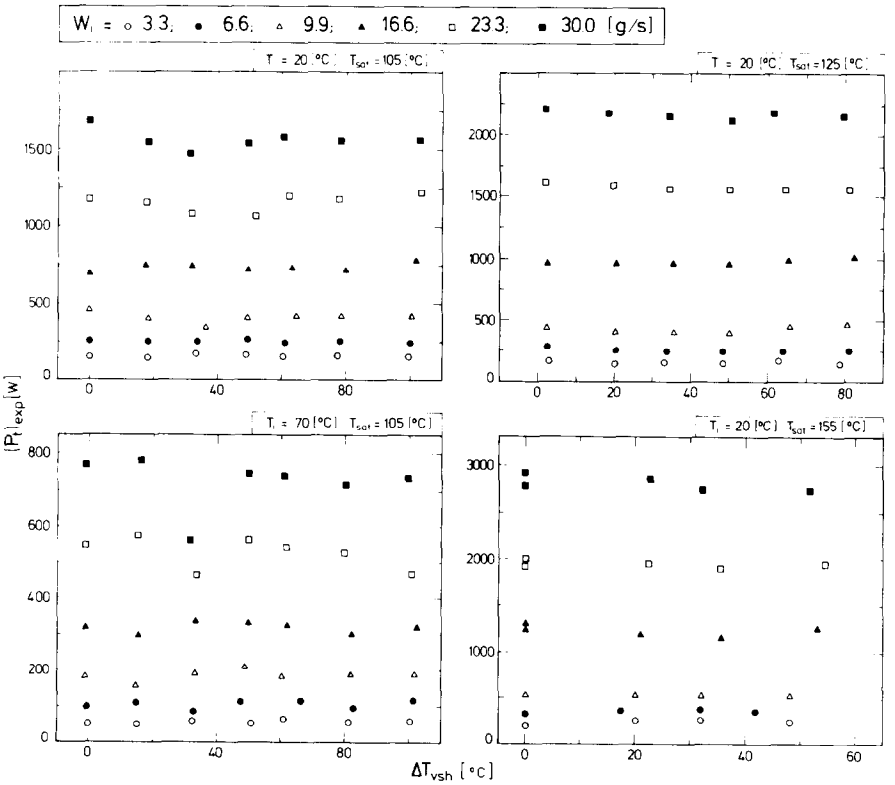

FIG. 7. Total thermal power (experimental) vs degree of steam superheating.

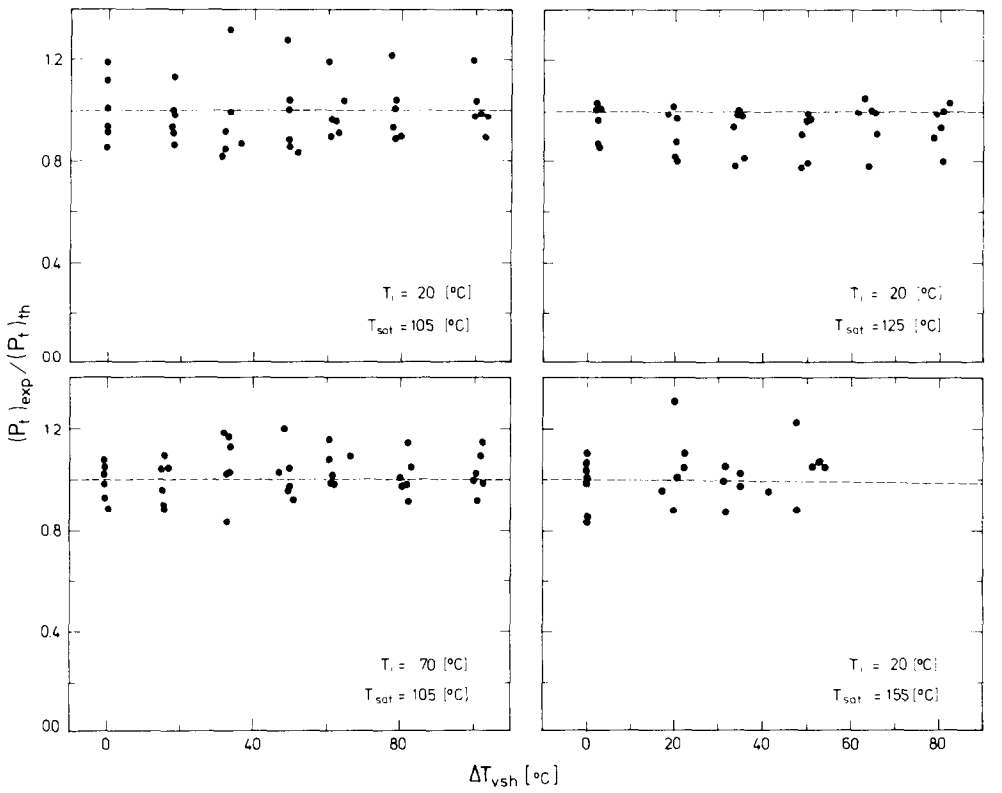

FIG. 8. Comparison between total thermal power from experimental data (superheating conditions) and model predictions [15] (saturation conditions), vs degree of steam superheating.

and steam thermodynamic conditions and of inlet water mass flow rate.

Such a confirmation enables the prediction of the total heat transfer between superheated steam and subcooled water in direct contact, on the basis of available correlations and models for direct contact condensation of saturated steam on water.

Referring to the tested geometry, the authors proposed a theoretical model [15] for the description of direct contact condensation of saturated steam on subcooled water.

A comparison between the total power experimental data (referred to superheated steam conditions) and model predictions (referred to saturation conditions) is reported in Fig. 8. An overall representation of the comparison is plotted in Fig. 9. The agreement is well within a $\pm$ 20% band from model predictions line, independent of the inlet water mass flow rate value. It is worth saying that, from propagation analysis errors, the accuracy in P_t determination, from temperature and water mass flow rate measurements, turns out to be evaluated in a $\pm$ 20% band. Model predictions lie within the experimental accuracy.

The experimental confirmation of the theoretical considerations proposed in Section 3 enables us to express the total heat transfer coefficient according to equation (9), i.e.

$$h_t = P_t/S(T_{sat} - T_i). \quad (9)$$

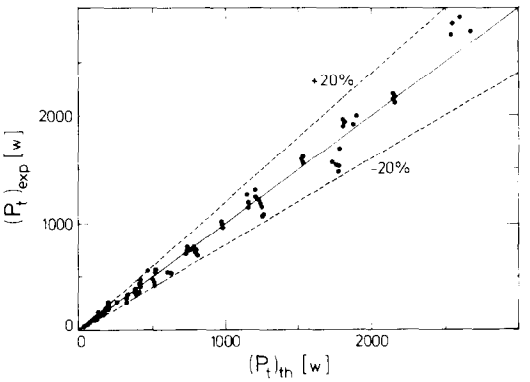

FIG. 9. Comparison between total thermal power from experimental data and model predictions [15].

The total heat transfer coefficient, h_t, like the total thermal power, P_t, is not dependent on superheated steam temperature.

Experimental data of h_t, compared with theoretical model predictions (referred to saturation conditions), are reported in Fig. 10 (vs steam superheating) and in Fig. 11 (as an overall representation). From these two plots it can be seen that the agreement between experimental data and model predictions is appreciably within the experimental accuracy, i.e. $\pm$ 20%.

As far as the condensation heat transfer coefficient is concerned, this is obtained, knowing h_t, from

$$h_c = \lambda h_t/[\lambda + c_{pv}(T_{vsh} - T_{sat}) + c_{pl}(T_{sat} - T_0)]. \quad (12)$$

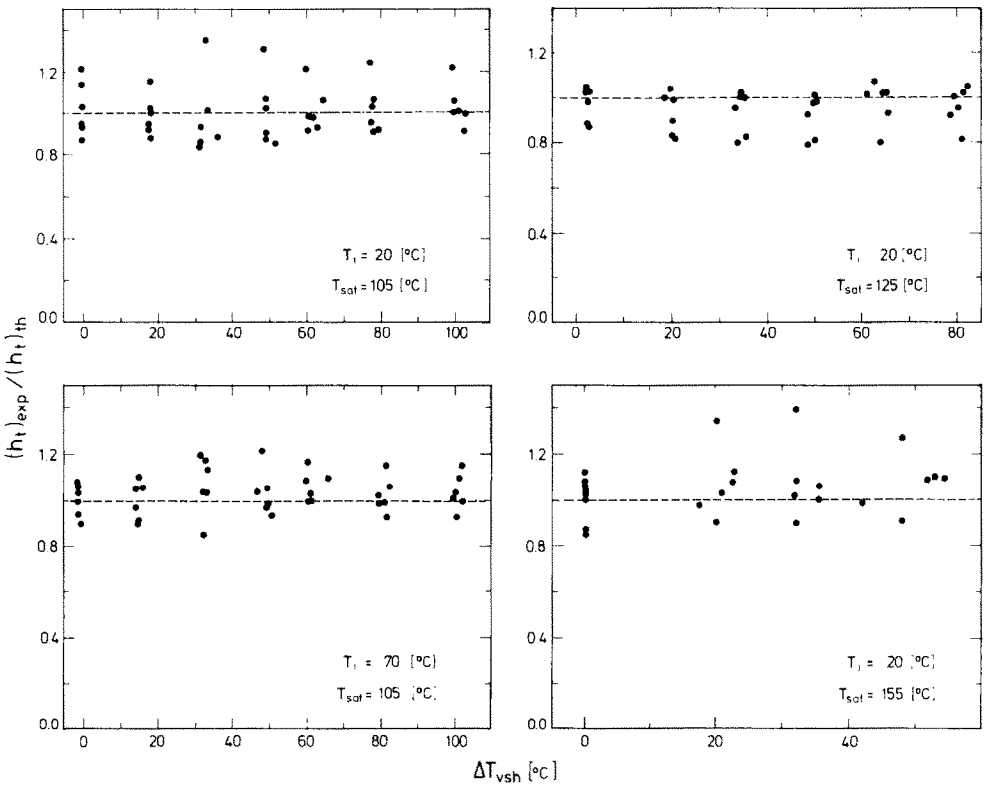

FIG. 10. Comparison between total heat transfer coefficient from experimental data (superheating conditions) and model predictions [15] (saturation conditions) vs degree of steam superheating.

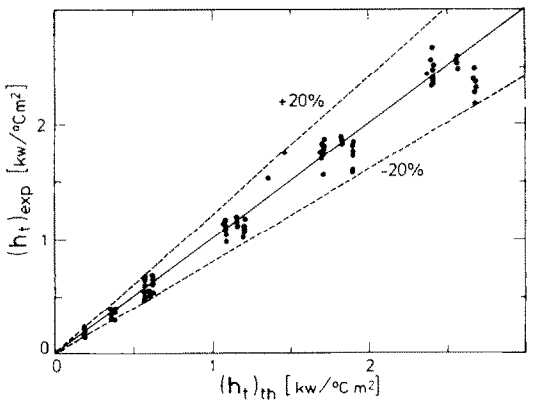

FIG. 11. Comparison between total heat transfer coefficient from experimental data and model predictions [15].

However, it must be pointed out that, within the investigated ranges of steam superheating, T_{vsh}, and pressure, p, the influence of T_{vsh} on h_c is not so high because $c_{pv}(T_{vsh} - T_{sat})$ is always much less than $\lambda + c_{pl}(T_{sat} - T_o)$.

Experimental determinations of h_c are reported in Fig. 12, together with the model predictions, vs steam superheating. Concerning h_c predictions, according to equation (12), knowledge of both h_t and outlet water temperature, T_o, is necessary. Values for both of these are supplied by the theoretical model proposed by the authors [15]. The agreement between experimental data and model predictions is essentially good, except for a few cases, even though the maximum difference is below $\pm$ 25%.

Finally, in Fig. 13—as is Fig. 12—the experimental value of condensed mass flow rate, W_c, is plotted vs the degree of steam superheating, ΔT_{vsh}, together with the model predictions. Concerning the latter, they refer to P_t and T_o predictions, whilst W_c is computed by means of equation (10). Concerning the agreement, the same considerations drawn for the h_c prediction are valid.

6. CONCLUDING REMARKS

The results of an experiment performed with superheated steam (quasi-stagnant conditions) and subcooled water (slowly moving) in direct contact are presented, with particular reference to the analysis of the degree of superheating influence on heat and mass transfer in direct contact condensation. The experimental results confirm the theoretical considerations proposed by the authors:

(a) the total thermal exchanged does not depend on the degree of steam superheating;

(b) it is meaningful to consider as a 'driving force', for the total heat transfer coefficient, the difference between saturated steam temperature, T_{sat}, and the

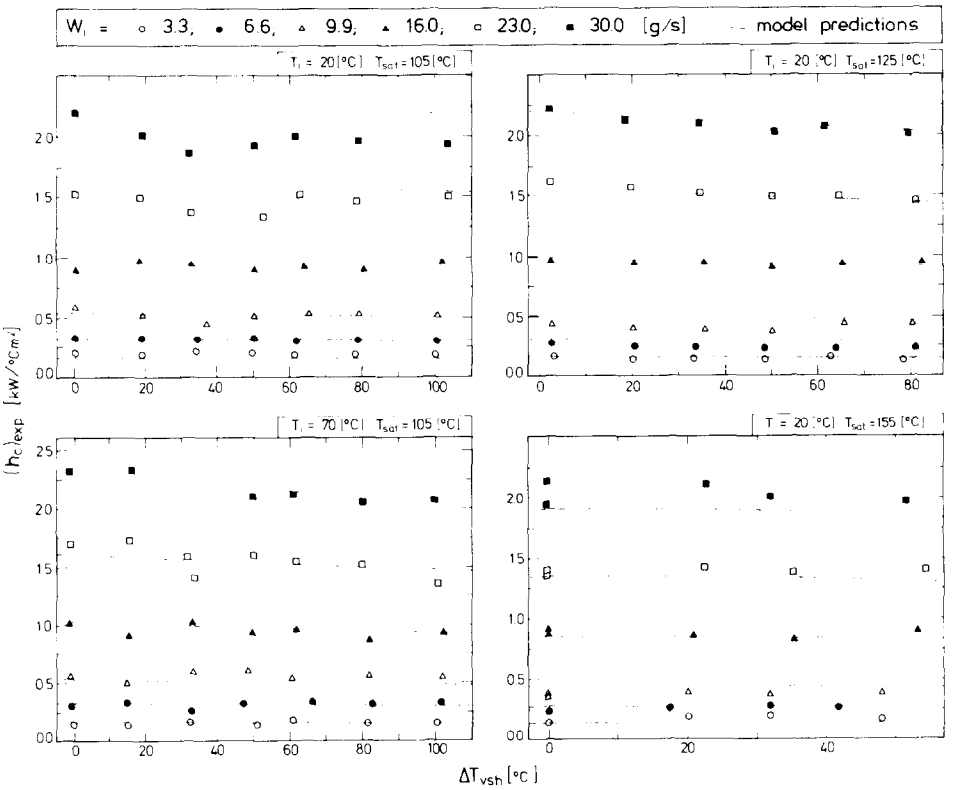

FIG. 12. Comparison between condensation heat transfer coefficient from experimental data (superheating conditions) and model predictions [15] (saturation conditions) vs degree of steam superheating.

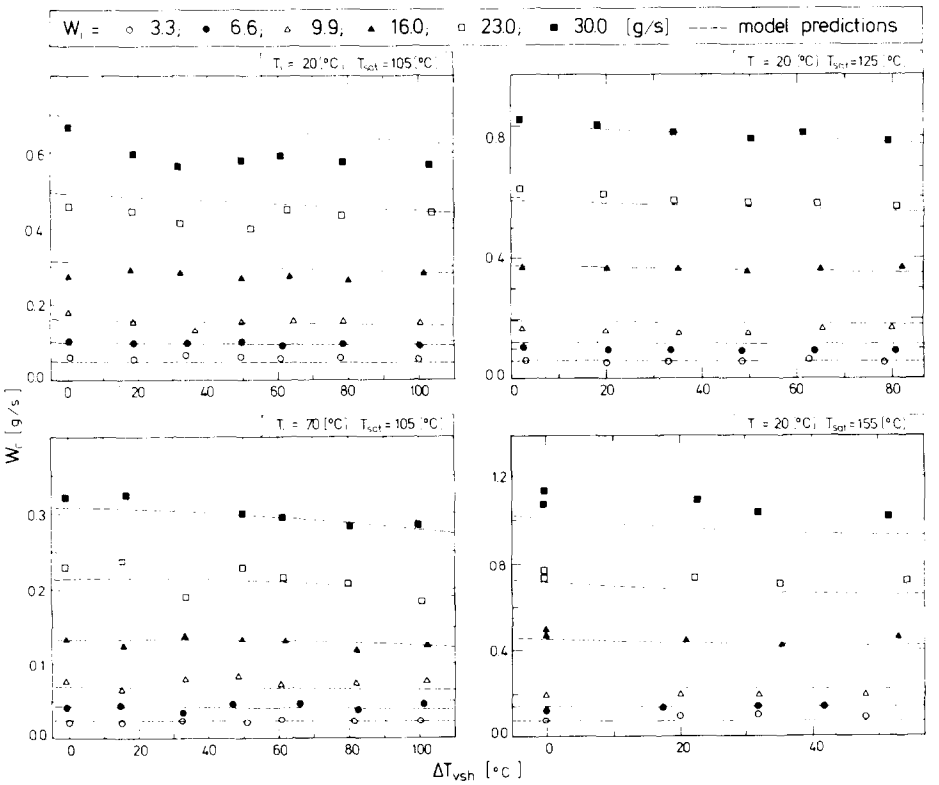

FIG. 13. Comparison between condensed mass flow rate from experimental data (superheating conditions) and model predictions [15] (saturation conditions) vs degree of steam superheating.

bulk water temperature, T_b, or the inlet water temperature, T_i ($T_i \simeq T_b$).

The total heat transfer coefficient, h_t, is therefore predictable by means of correlations or models valid for 'saturated steam'.

The condensation heat transfer coefficient, h_c, is, on the other hand, dependent on the degree of steam superheating (h_c decreases with ΔT_{vsh}).

A good agreement shows the comparison between experimental data (h_t, h_c) and predictions obtained with a theoretical model proposed by the authors [15] on the basis of a previous experiment with saturated steam.

Acknowledgements—The authors wish to express their gratitude to Mr N. Ciotti who performed the experimental runs and gave useful suggestions. Much is due to the helpful assistance offered by Mr F. Binello and Mrs B. Perra in the editing of this paper.

REFERENCES

1. G. P. Celata, M. Cumo and G. E. Farello, Direct contact condensation of steam on slowly moving water, III, International Topical Meeting on Reactor Thermal Hydraulics, Newport, Rhode Island, 15–18 October (1985).
2. E. M. Sparrow and J. L. Gregg, A boundary layer treatment of laminar film condensation, *J. Heat Transfer* **21**, 13–18 (1969).
3. S. G. Bankoff and H. J. Kim, Countercurrent steam–water flow in a flat plate geometry, Rept NU-8201B, Chem. Engng Dept., Northwestern University, Evanston, Illinois (1982).
4. S. G. Bankoff and H. J. Kim, Local heat transfer coefficient for condensation in stratified countercurrent steam–water flows, ASME Paper No. 82-WA/HT-24 (1982).
5. S. G. Bankoff and H. J. Kim, Local condensation rate in nearly horizontal stratified countercurrent flow of steam and cold water, *A.I.Ch.E. Symp. Ser.* 225 **79**, 209–223 (1983).
6. L. K. Brumfield, R. N. Houze and T. G. Theofanus, Turbulent mass transfer at free, gas–liquid interfaces with application to open channel, bubble and jet flows, *Int. J. Heat Mass Transfer* **19**, 613–624 (1976).
7. L. K. Brumfield, R. N. Houze and T. G. Theofanus, Turbulent mass transfer at free, gas–liquid interfaces, with application to film flows, *Int. J. Heat Mass Transfer* **18**, 1077–1081 (1975).
8. J. H. Linehan, The interaction of two-dimensional stratified, turbulent air–water and steam–water flows, Ph.D. thesis, Dept. of Mech. Engng, University of Wisconsin (1968).
9. R. M. Thomas, Condensation of steam on water in turbulent motion, *Int. J. Multiphase Flow* **5**, 1–15 (1979).
10. W. Kirchner and S. G. Bankoff, Condensation effects in reactor transients, *Nucl. Sci. Engng* **89**, 310–321 (1985).
11. J. A. Block, Condensation-driven fluid motions, *Int. J. Multiphase Flow* **6**, 113–129 (1980).
12. D. H. Rooney, H. C. Simpson, A. M. Bradford and E. W. Bessada, Non-equilibrium effects in direct contact condensation under countercurrent flow, European Two-phase Flow Group Meeting, Eindhoven, 2–5 June (1981).
13. D. H. Rooney and H. C. Simpson, Further studies of non-equilibrium during refill in a PWR, European Two-phase Flow Group Meeting, Zurich, 14–17 June (1983).
14. S. G. Bankoff, Some consideration studies pertinent to LWR safety, *Int. J. Multiphase Flow* **6**, 51–67 (1980).
15. G. P. Celata, M. Cumo, G. E. Farello and G. Focardi, A theoretical model of direct contact condensation on horizontal surface, ENEA Report RT/TERM 86/1 (1986).

CONDENSATION PAR CONTACT DIRECT DE LA VAPEUR D'EAU SURCHAUFFEE AVEC L'EAU LIQUIDE

Résumé—On présente et on discute les résultats d'une recherche expérimentale sur l'interaction de la vapeur d'eau surchauffée (pratiquement stagnante) avec de l'eau froide (légèrement mouvante). Comme prévu dans une étude théorique, la puissance thermique totale (et par conséquent le coefficient de transfert thermique total) ne montre pas une dépendance sensible vis-à-vis de la température de surchauffe de la vapeur et elle peut être pratiquement évaluée au moyen des formules existantes pour les conditions de vapeur saturante. Le coefficient de transfert thermique par condensation en contact direct est faiblement fonction du degré de surchauffe de la vapeur, comme cela est confirmé expérimentalement.

DIREKTKONTAKT-KONDENSATION VON ÜBERHITZTEM DAMPF IN WASSER

Zusammenfassung—Mit Hinblick auf die Wechselwirkung zwischen überhitztem Dampf (praktisch ruhend) und unterkühltem Wasser (langsam fließend) werden die Ergebnisse einer experimentellen Untersuchung vorgelegt und diskutiert. Wie in einer theoretischen Untersuchung vorausgesagt, zeigt die thermische Gesamtleistung (und entsprechend der Gesamtwärmeübergangskoeffizient) keine merkliche Abhängigkeit von der Temperatur des überhitzten Dampfes, so daß sie praktisch mit verfügbaren Beziehungen für Sattdampfbedingungen berechnet werden kann. Der Wärmeübergangskoeffizient bei der Direktkontakt-Kondensation ist an den Gesamtwärmeübergangskoeffizienten gekoppelt und hängt schwach vom Überhitzungsgrad ab. Dies wurde im Versuch bestätigt.

КОНДЕНСАЦИЯ ПЕРЕГРЕТОГО ПАРА НА ЖИДКОСТИ ПРИ НЕПОСРЕДСТВЕННОМ КОНТАКТЕ

Аннотация—Приведены результаты экспериментального изучения взаимодействия практически неподвижного перегретого пара с медленно движущейся недогретой жидкостью. Как и предполагалось в теоретическом исследовании, общая тепловая мощность (и, соответственно, суммарный коэффициент теплообмена) не зависит от температуры перегретого пара, поэтому она может быть оценена из соответствующих уравнений. Коэффициент теплообмена при контактной конденсации сильно зависит от суммарного коэффициента теплообмена и, что подтверждено экспериментом, слабо зависит от степени перегрева пара.